

Isotopic production cross sections of fragmentation residues in reactions induced by $^{238}\text{U}(1\text{ A} \cdot \text{GeV})$ in deuterium

E. Casarejos^{a*}, P. Armbruster^b, J. Benlliure^a, M. Bernas^c, A. Boudard^d, S. Czajkowski^e,
T. Enqvist^b, R. Legrain^d, S. Leray^d, B. Mustapha^c, M. Pravikoff^e, F. Rejmund^c,
K.-H. Schmidt^b, C. Stephan^c, J. Taieb^c, L. Tassan-Got^c, C. Volant^d, W. Wlazolek^b

^a Universidad de Santiago de Compostela, E-15782 Santiago de Compostela, Spain

^b Gesellschaft für Schwerionenforschung, GSI D-64291 Darmstadt, Germany

^c Institute de Physique Nucléaire, IPN F-91406 Orsay cedex, France

^d DAPNIA/SPhN, CEA/Saclay, F-91191 Gif sur Yvette cedex, France

^e CENBG , F-33175 Gradignan cedex, France

Abstract

More than 500 isotopic production cross sections of fragmentation residues produced in the reaction of $^{238}\text{U}(1\text{ A} \cdot \text{GeV})$ in deuterium were measured with high accuracy. The experimental technique that allows the unambiguous identification is reviewed. The characteristics of the reaction we study, the high fissility of the ^{238}U and the impact of two nucleons, are discussed in respect to other available experimental data. These data allow the study of the fission and fragmentation reaction mechanisms involved in relativistic heavy ion collisions. The results from representative models describing the process are compared with the data. This comparison will allow to improve the understanding of the the reactions mechanisms involved.

1 Introduction

A large experimental program was initiated at GSI in 1996 to determine the production cross sections of heavy residues in relativistic heavy-ion collisions [1]-[6]. The goal of the program was to provide relevant nuclear data for *accelerator-driven reactor systems* ADS [7, 8]. The project aimed the study of the fission and fragmentation reaction mechanisms involved in relativistic heavy ion collisions, defining a large benchmark data collection. Spallation reactions are understood as a two-step process [9]. The impact of a light nucleus (or nucleon) into a heavy target nucleus induces a certain *pre-equilibrium emission*, and the formation of an excited *pre-fragment*. The further de-excitation of the pre-fragment either by particle emission or fission, the second step, defines the reaction mechanism leading to the residue.

These data provide basic information for intense neutron sources, needed for material science investigation, and in technical application as those of the ADS. The production of intense *radioactive ion beams* is nowadays feasible using *isotope separation on-line* ISOL techniques, based on spallation reactions [10]. The production of either neutron deficient or neutron rich

*corresponding author: casarejo@usc.es

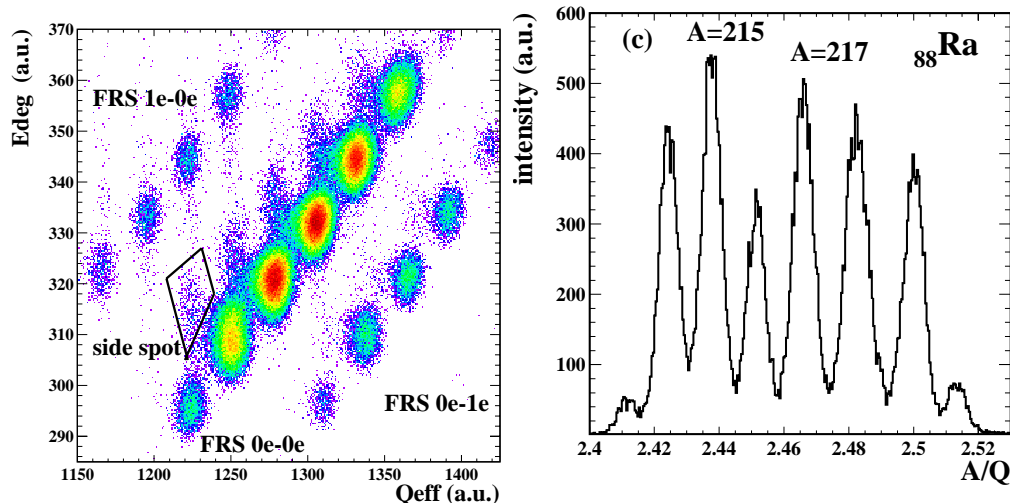


Figure 1: **Left panel:** Energy loss measured after the change in magnetic rigidity before and after the degrader, vs. the energy loss measured with the two ionisation chambers (both in arbitrary units). The FRS spectrometer was adjusted to centre the isotope ^{195}Pb , with the corresponding energy after the reaction. The most populated spots correspond to those nuclides which are always bare along the spectrometer. The spots above and below the former ones, correspond to those nuclides with one electron before the degrader and bare after, and vice-versa, respectively. The most unfavourable case, that of a nuclide with one electron unchanged, is also separated in the less populated spots next to the main line. **Right panel:** Production rate (arbitrary units) of different isotopes of the element Ra . The mass number is indicated for two of them.

nuclides is very much constrained by the available intensities and the reactions mechanisms. The correct evaluation of those productions will allow to increase the present understanding of the reaction mechanisms and improve the expected intensities. Additionally, spallation produces excited nuclear matter at normal densities while keeping low the angular momentum. Those are conditions allowing to investigate the onset of thermal multifragmentation.

The complete isotopic distributions of fragmentation residues of the reactions induced by 2 GeV deuterons in ^{238}U were measured [6], and some results are discussed in this work. The experiment was performed in *inverse kinematics*, using a $1\text{ A}\cdot\text{GeV}$ beam of ^{238}U and a target of liquid deuterium. The primary reaction products were fully identified in mass and atomic number prior to beta decay, using the *fragment separator* FRS. This technique allows an unambiguous identification of the residues [11]. This kind of studies give access directly to the primary reaction production, thus allowing the study of the reaction mechanisms.

The comparison of the data presented here with related data recently available helps in the understanding of the features of the two reaction mechanism involved. ^{238}U is the heaviest stable ion we can accelerate. It is a deformed nucleus and has a high fissility. The deuterium is the simplest extension to single-nucleon collisions and presents a wide spatial distribution. The reaction studied allows us to discuss the influence of the additional energy in respect to nucleon induced collisions, the geometry of the impact, or the strength of the fission channel. Different simulation codes pursue in the description of the reaction process and the evaluation of the cross sections. Despite their capacity to describe the general trends of the measured data, these codes

present a poor predictive power [12, 13]. In order to be used in many relevant applications of the implicated reactions, mostly for *accelerator driven systems* and *radioactive ion beams*, the codes have to be improved. The use of a deuteron target provides a link in between reactions induced by protons and ions. A satisfactory description of these steps will help to improve the existing codes in short-term.

2 Experimental technique

The experiment was performed at GSI by shooting a ^{238}U -beam accelerated in the SIS synchrotron up to $1\text{ A}\cdot\text{GeV}$, into a cryogenic liquid-deuterium target with a thickness of 200 mg/cm^2 . The cryogenic target was used for the first time in this kind of experiments, allowing the access to proton and deuteron induced reactions. The deuterium is encapsulated within a structure made of Al and Ti to preserve the vacuum of the beam and residues line. The beam intensity, up to 10^8 particles/s, was measured continuously by a *secondary electron transmission monitor* SEETRAM [14], as well as the dead-time of the acquisition ($< 20\%$). The produced residual nuclides were fully identified in mass and atomic numbers, while flying forward, using the *FRAGMENT Separator* FRS [15], a 70 meters long, zero-degree magnetic spectrometer, and a dedicated detection setup. This technique, so called *inverse kinematics*, allowed us the measurement of a large amount of high-quality data in a single experiment. The separation of the heavy residues with good resolution $A/\Delta A \sim 400$, is a very exigent technique, being possible with the *FRS*, which has an angular acceptance of 15 mrad , a longitudinal-momentum acceptance of 3% , and a resolving power of 1600, and was used as an achromatic energy-loss spectrometer.

Two plastic scintillators, two ionisation chambers and two multi-wire proportional chambers, were used to provide information on position and energy losses of the residues in-flight. The short times of flight involved ($< 200\text{ ns}$) allowed to observe the primary production of the reaction, overcoming the radioactive decay drawback present in direct kinematic experiments [16]. Only a few extremely short-lived alpha-emitters with 128 neutrons, having half-lives around 100 ns , partly decayed inside the spectrometer. For all other nuclides, the production cross sections were determined prior to their radioactive decay.

The beam allowed the calibration of the involved detectors (for time, energy loss, and particle counting), the ion-optical parameters of the FRS, and the thicknesses of the layers of matter present in the path of the residues. The measurement of the magnetic fields of the FRS and the position of the particles in the magnetic dispersion coordinate at the focal planes of the FRS, defines the magnetic rigidity $B\rho$ of each residue. Their time of flight defines the relativistic $\beta\gamma$ value. The definition of the ionic charge Q to mass A ratio of each residue is done according to the relationship $B\rho = A/Q \cdot \beta\gamma$. The proper assignation of ionic charge Q and atomic number Z is a challenge for nuclides with Z above 70, since the ionic state of a nucleus after traversing any layer of matter (as those of the target and the detectors) may change. At about $1\text{ A}\cdot\text{GeV}$, ^{238}U presents mainly three ionic states, being bare ions the most populated. The distribution depends strongly on Z number. On the one hand, the measurement of charge with one ionisation chamber does not provide Z straightforward, due to the lack of resolution for the highest charges, and because the sensitivity to Q instead of Z in the detection process. On the other hand, we must know the charge Q within the spectrometer to define correctly the nuclide mass from the magnetic rigidity value.

Using the uncorrelated signals from two ionisation chambers (a Nb stripping foil 230 mg/cm^2 thick was put in between) the Z number was assigned, according the observed energy loss. By

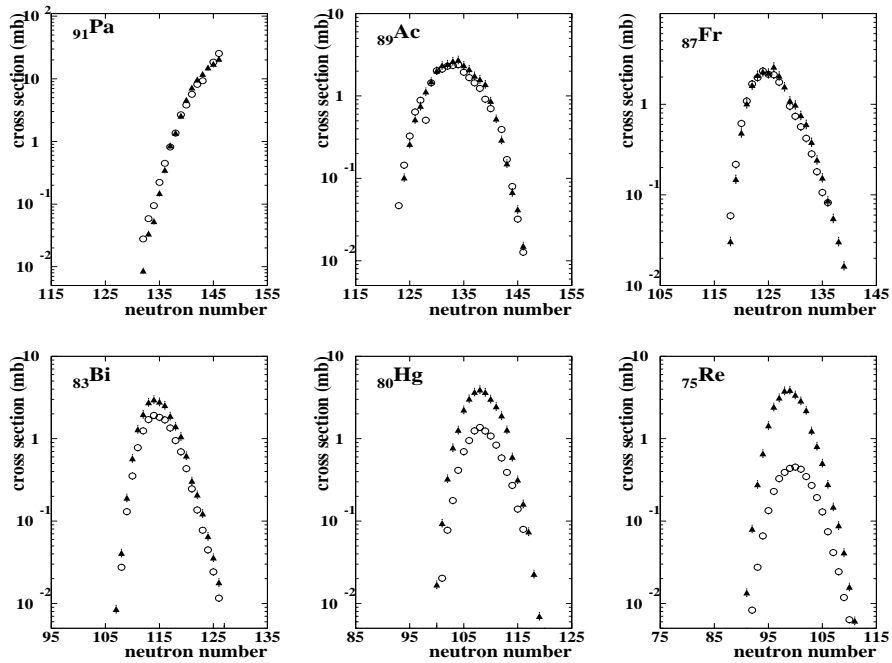


Figure 2: Isotopic cross sections of residues of the reaction induced by $^{238}\text{U}(1\text{ A} \cdot \text{GeV})$ in deuterium (full symbols, this work) and proton (open symbols,[5]), for elements $_{91}\text{Pa}$, $_{89}\text{Ac}$, $_{87}\text{Fr}$, $_{83}\text{Bi}$, $_{80}\text{Hg}$, $_{75}\text{Re}$. The error bars are visible if larger than the symbol size.

selecting the maximum energy loss observed in the two chambers, the value will correspond to the Z value, since the probability of being bare at least in one chamber is maximum.

Additionally the electromagnetic energy loss induced by a profiled achromatic Al *degrader* ($\sim 4\text{ g/cm}^2$) in the intermediate focal plane of the FRS, allowed alternatively the definition of the ionic charge of the nuclide. The *degrader* [17] is a dedicated device which keeps the achromaticity of the spectrometer. The change in magnetic rigidity before and after the degrader, gives a measurement of the energy loss, thus of the ionic charge Q of the particle. Two Nb stripping foils were installed after the target (60 mg/cm^2) and after the degrader (105 mg/cm^2), to enhance the fraction of fully stripped ions along the spectrometer.

The comparison of the measurements obtained from the ionisation chambers and the degrader, as shown in Fig. 1, defines the ionic charge of the nuclides at different positions of the setup. The events with a correct Z assignation with the ionisation chambers lie on the spots of the three parallel lines visible on the figure. The most populated spots correspond to those nuclides which are always bare along the spectrometer. The spots above and below the former ones, correspond to those nuclides with one electron before the degrader and bare after, and vice versa, respectively. The most unfavourable case, that of a nuclide with one electron unchanged, is also separated in the less populated spots next to the main line. These small spots also contain those events with a wrong Z assignation by the ionisation chambers. Other cases are negligible. Additionally the resolution to separate the different charges is improved.

With this procedure we demonstrate that the isotopic identification is fully unambiguous. The degrader is a key piece when working with heavy nuclides, since it allows the unambiguous separation of the different ionic charges. For residues with Z below 70, the identification needs

no more the degrader setup. We have used the two procedures for Z above 70, and we have checked the agreement of the two independent results. The quality of the final separation of the isotopes is shown in Fig. 1, right panel.

3 Cross sections

To define the production cross sections we had to correct the measured counting rates of each identified nuclide for the different effects inherent to our method, previous to the normalisation to the target thickness and beam intensity. The dead time of the whole acquisition system was monitored with an accuracy within 1%. The uncertainty in beam intensity is 4% after the calibration of the SEETRAM. The uncertainty in the target thickness was calculated including the deformation of the target walls, resulting in 3%. The statistical accuracy was kept well below 5% for most of the nuclides, and the productions were measured above 0.01 mb. An additional test of the statistical accuracy was done by comparing the measured cross-sections of nuclides along paths of the chart of nuclides with a softer change than that of the isotopic chains. We have used, e.g. the chains following the $N-Z=\text{constant}$ relationship. The deviation of any measured production from the smoothed trend observed, induces a correction. It was found that this correction was rather tiny, showing the statistical quality of the data, as shown in the smoothness of the isotopic cross sections in Fig. 2.

The limited momentum acceptance of the spectrometer is overcome by overlapping several magnetic settings, which scan the whole longitudinal momentum distribution for each nucleus. The transversal distributions, of few mrad, are fully accepted. The momentum transmission is then 100%, with an accuracy within 1%, in the mass range we have considered.

The momentum scanning was designed to recover the momentum distributions of all the bare nuclides produced. It means that we have selected only the nuclides belonging to the main spots in a plot as that of Fig. 1. To correct the observed production we had to evaluate the probability of having bare ions along the FRS, as well as within the two ionisation chambers. The evaluation was done according a *three states method* [18], since at our energies the bare, hydrogen-like and helium-like states are the only populated states. The calculations were cross checked with values we measured in our system, and the uncertainty established in 5%.

The secondary reactions in any layer of matter along the path of the detection, change the production intensity of any nuclide. The setup and identification method guarantee that this secondary production does not contaminate any other residue. Thus we have to correct the production of each nucleus according the losses in all the matter traversed. Both, nuclear [19, 20] and electro-magnetic-dissociation [21, 22] processes have been considered in the evaluation of the total reaction cross section. For the former process is evaluated with a microscopic Glauber-like method. The later process, is evaluated by considering the virtual photon field equivalent to the target nucleus, and the photon absorption cross section of the projectile. The losses in the degrader amount up to $\sim 40\%$ for the heavier residues. The cross section values for these processes were obtained with an accuracy of 10%.

With the former corrections we can evaluate the production of the whole target assembly. To subtract the production related to the Al, Ti and Nb components present at the target area either as layers of the target structure, or as strippers, we have used the production evaluated with reliable simulation codes. These values were cross checked with a set of measured data obtained with an empty target container. The productions observed due to those additional materials were typically below 3%. A safe uncertainty assigned to the code evaluations to

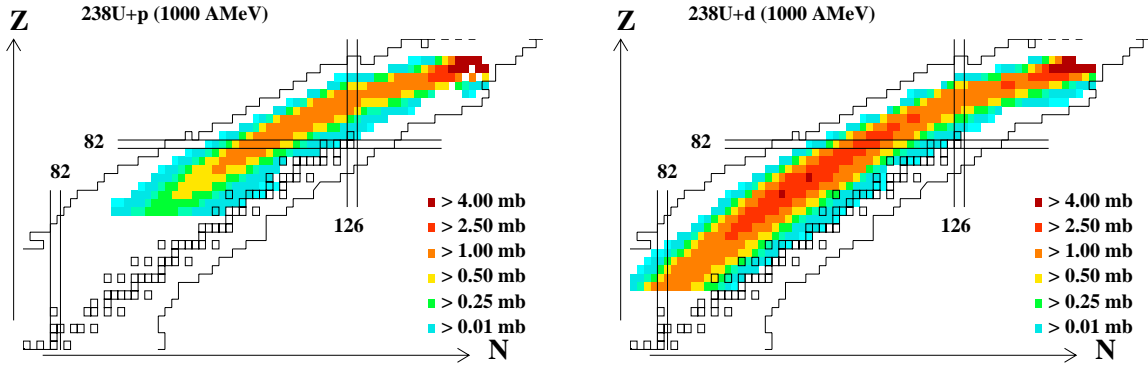


Figure 3: Production cross sections measured in the $^{238}\text{U}(1A \cdot \text{GeV})$ induced reactions on proton (left panel, [5]) and deuteron (right panel, this work), plotted in grey-scale on top of a chart of nuclides.

provide the values within a factor of two, induce a rather low uncertainty on the final values.

The observed yields suffer additionally from multiple reactions happening within the deuterium itself. The resulting production we have observed is then a redistribution of the primary production we aimed to measure. The possibility to correct the measured values relies in a realistic evaluation of the production cross section values of any residue within the deuterium, according to the method described in [1]. This correction includes both, the attenuation of the beam (and residue) flux within the target ($\sim 8\%$), and the additional contributions from other nuclides (increasing for lower masses). The resulting uncertainty of the cross-section values was 15-20%, depending on the mass.

4 Results

In this work we have measured more than 500 isotopic cross sections. The quality and quantity of the data which is now available allow to investigate the differences in respect to related reactions already investigated. In Fig. 3 we show the cross-sections values measured in the ^{238}U induced reactions on proton (left panel, [5]) and deuteron (right panel), plotted in grey-scale on top of a chart of nuclides. The production of any residue is determined by the competition among the open de-excitation channels, mostly neutron, light-charged particles, and fission. Actually the fission channel will determine the production of residues of elements with Z above 80. Below that limit, that channel is weakly populated, and the production lies in the so called *fragmentation corridor*, defined by the competition of proton and neutron emission, thus along the neutron deficient side. We observe in Fig. 3 that the position of the *corridor* is common to proton and deuteron systems, as expected in the *limiting fragmentation regime*. However the corridor is larger in the case of the deuteron residues. This effect is due to the additional available excitation energy in the system, just after the collision. The de-excitation can proceed thorough larger evaporation chains, reaching lighter residues.

In Fig. 2 we show the isotopic distribution of residues from the reactions induced $^{238}\text{U}(1A \cdot \text{GeV})$ in proton (open symbols, [5]) and deuteron (full symbols), for some elements. Residues close to the projectile show a production rather similar in both reactions. This observation can be explained if we consider that the heaviest residues result from the most peripheral collisions. Due

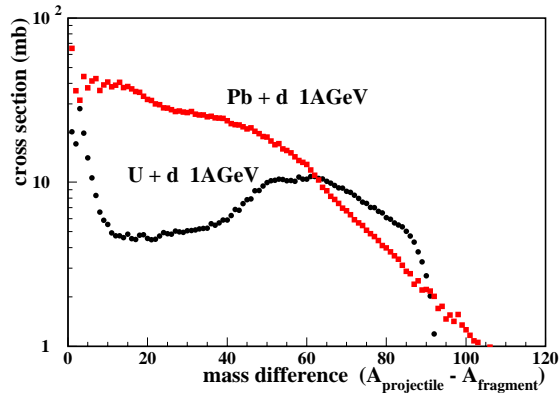


Figure 4: Mass distribution of production of residues in the reactions induced by ^{208}Pb [2] and ^{238}U (this work) on deuteron, as a function of the difference in mass of the residue in respect to the projectile.

to the large spatial distribution of the deuteron, many of the impacts involve a single nucleon. Thus both reactions, with deuteron and proton, result in the same production. Consequently, no differences between neutron and proton impacts were found. For elements with Z below 80 the production by deuteron is higher than that by proton.

In Fig. 4 we compare the isobaric distribution of production of residues in the reactions induced by ^{208}Pb [2] and ^{238}U on deuteron, as a function of the difference in mass of the residue in respect to the projectile. As known from other spallation reactions [3], the results are expected to be similar, just scaled by the ratio of the total reaction cross sections. However large differences in the production of heavy residues were observed, due to the fission channel. This channel largely dominates the reaction mechanism in the neighbourhood of the projectile ^{238}U , depopulating the production of residues close to the projectile and populating medium-mass residues.

5 Model calculations

The models describing spallation reactions are based on the two-step scheme, with dedicated codes for each part. The formation of the pre-fragment is described as an *intranuclear cascade* INC, triggered by the impact of the nucleons of the projectile with those of the target. During this fast process some nucleons may be ejected (*pre-equilibrium emission*), and the remaining excited nucleus constitutes the so called pre-fragment. Typical INC models are those of ISABEL [23, 24] (after VEGAS and Bertini's cascades), and the INC of Liège INC-L [25]. INC codes share common grounds: monte-carlo calculation, time-like evolution, semi-classical collision description, ... Nevertheless the two codes propose completely different approaches to the problem. While the nucleons which have not yet collided are treated as a continuum Fermi-sea by ISABEL, they are treated as separated units by INC-L.

The de-excitation of the pre-fragment is typically implemented by considering a sequential de-excitation process, in each step evaluating the probabilities for all open channels [26]. Those channels determine the reaction mechanism leading to a residue: namely particle emission and

fission, being also possible the sequential presence of both. Alternative mechanisms as *multi-fragmentation* are of minor interest in our case: according to the energies present in the reaction, the multi-fragmentation channel would poorly contribute to the production, in respect to the total reaction cross section, and being negligible for heavy residues. The discussion is beyond the scope of our work. The pre-fragment is usually described as a compound nucleus, thus the de-excitation description adopted is the statistical one. The available models differ in (i) the channels included, (ii) the approximations made to define the probabilities of the channels, (iii) the parameterisation of the different magnitudes involved in the evaluation of the probabilities. The code we have used in the so called ABLA [27], that has been demonstrated to be well suited for the description of the residues of relativistic heavy-ion reactions [27].

The code ABLA includes the neutron, proton and alpha particle emission, and fission. The emission is described in a Weisskopf-like formulation. The probability for each channel is defined according the ratio of the phase space (level density ρ) after and before the emission. The level densities ρ are functions strongly dependent on the excitation energy U ($\rho \propto e^{\sqrt{aU}}$). The level density parameter a , relating temperature T and energy $U = aT^2$, is given according to Ref. [28]. The separation energy of the nucleons is defined according the finite-range liquid drop model [29]. The proton and alpha Coulomb barriers are parameterised to include the effects of tunnelling [30]. Fission probability is described in ABLA following the Borh-Wheeler formalism and according to the Moreto description [31]. Again the ratio of level densities define the probability, but in this case the energy of the final state is evaluated above the fission barrier [32]. The fission residue distribution is defined from a semi-empirical model, well adapted to the description of the data of mass and charge distributions available [33].

In Fig. 5 we show the isotopic distribution of several elements, in the reactions induced by ^{208}Pb (upper panels, [2]) and ^{238}U (lower panels) on deuteron, both at $1\text{ A} \cdot \text{GeV}$. The lines are the results of the calculations obtained by coupling the INC models ISABEL (full line) and INC-L (dotted line), to ABLA.

In the right-most panels we show residues far from the projectile. Since they correspond to the longer de-excitation chains, their final production is dominated by the second step of the reaction. The competition of the different processes define the position of maximum production, shape and width of the distribution. We observe that, despite the correct shape, the calculations underestimate the the measured data. This is a common drawback from the two INC cascades, which do not populate sufficiently the high-energy tail of the excitation energy function.

However, heavier residues as those shown in the central panels, are well reproduced. Now the description of the INC+ABLA system is shown to be adequate. Since the fission channel is weak for the ^{208}Pb residues, we conclude that the competition of proton-neutron emission is well described in ABLA. Also ^{238}U residues are well reproduced, and the fission channel, not being very strong, is well resolved. We also note that the performance of the ISABEL code is better than that of the INC-L, as e.g. for element $_{79}\text{Au}$: the neutron rich isotopes are usually over-estimated by INC-L.

The production of residues close to the projectile (left-most panels) are well reproduced by the calculations for ^{208}Pb . It is not the case of ^{238}U : the production for neutron deficient isotopes is underestimated by the calculations. The effect seems to be related to the fission channel, whose description fails for isotopes with high fissilities. The disagreement found between the data and the results of the models, might indicate that the level density is not well described in the case of the heavier residues. That could be an effect of the double-barrier which show many deformed nuclides in that region. Otherwise it could also be an effect of collective excitations which around the shell of 126 neutrons has to be carefully treated (the collective effects were not

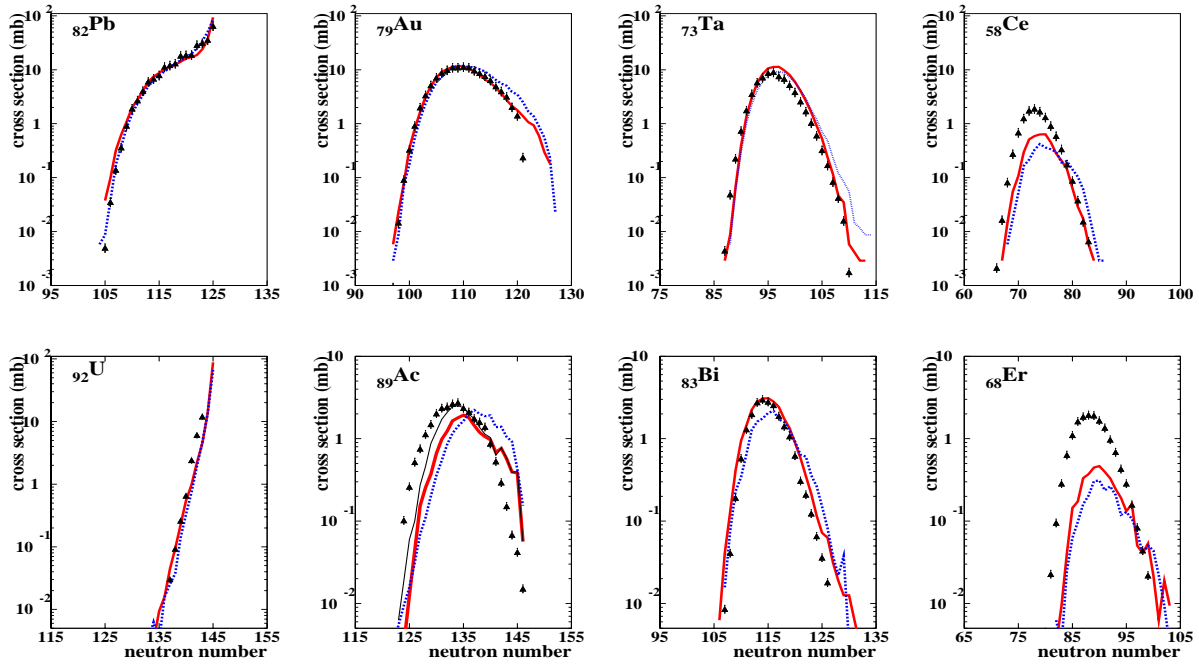


Figure 5: Isotopic distribution of production of residues in the reactions induced by ^{208}Pb (upper panels, [2]) and ^{238}U (lower panels) on deuteron, for elements closer-to-further of to the projectile in the left-to-right direction, corresponding to the same number of protons removed from the projectile. The lines correspond to calculations performed with the codes ISABEL (full line) and INC-L (dotted line), both coupled to ABLA (See the text for details). For element $_{89}\text{Ac}$ the thin full line corresponds to the result of ISABEL+ABLA, with fission barriers artificially increased by a 6%.

included in our calculations; it is feasible according the description given in Ref. [27]). Actually, changes of 5% in the value of the fission barrier are immediately reflected in the result of the model, as can be seen in Fig. 5 for the element $_{89}\text{Ac}$ (thin full line). These data will allow to further investigate the fission process.

The INC codes fail in the overall description of the production, since the high energy tail is not well reproduced. The code ABLA is capable to give a rather good description of the two reaction mechanisms present. Nevertheless a non appropriate description of the probability for the fission channel, results in a less accurate reproduction of those residues more affected (high-fissility isotopes).

6 Conclusions

We have measured more than 500 isotopic production cross sections from fragmentation residues of the reaction induced by of $^{238}\text{U}(1\text{ A}\cdot\text{GeV})$ in deuterium. The large collection of data recently available after the work developed by our collaboration, allows a systematic study of the reactions mechanisms which are present in these processes.

The deuteron data showed the influence of the larger energy available in the system, in respect to nucleon induced reactions . Longer de-excitation chains populated lower mass isotopes,

extending the fragmentation production to masses 100 units below that of the projectile. The difference in energy deposition between nucleon and ion collisions can also be investigated. We also showed how the strength of the fission mechanisms determines the production of heavy spallation residues. The range of impact parameters that enhance the probability of a single-nucleon collision of deuterium, showed that (i) no difference between proton and neutron impact was detected, and (ii) that proton and deuteron induced reactions share a common wide range of production due to the large spatial distribution of the deuterium.

The comparison of the results from proton and deuteron induced reactions will allow to improve the description of the impact of several nucleons, since the deuteron is the simplest extension after the collision of a single nucleon. We saw that the high energy range of the result from INC models is not well described. The adequate description of the energy distributions by one and two nucleons will help to better understand the process. The comparisons of reactions involving ions with very different fissilities, help to determine the accuracy of the competition of the fission to particle-emission. The lack of an adequate description by the models in the case of heavy isotopes with high-fissilities, may indicate that either the fission barriers or collective excitations have to be better described. A satisfactory description of the two steps of the reaction will help to improve the existing codes in short-term.

This work was partially supported by the European Commission under projects EC-HPRI-CT-1999-00001 and FIS5-1999-00150.

References

- [1] T.Enqvist et al., Nucl. Phys. A 686 (2001) 481
- [2] T.Enqvist et al., accepted for publication in Nucl. Phys. A
- [3] F.Rejmund et al., Nucl. Phys. A 683 (2001) 540
- [4] J.Benlliure et al., Nucl. Phys. A 683 (2001) 513
- [5] J.Taieb, Ph.D. Thesis presented at Universite de Paris Sud and U.F.R. Scientifique d'Orsay, France, Sep. 2000. IPN report IPNO-T-00-10.
- [6] E. Casarejos, PhD in the University of Santiago de Compostela, June 2001, edited at GSI (in press)
- [7] C.Rubbia et al., Rep. CERN-AT/95-44(ET), 1995
- [8] C.D.Bowman, Annu. Nucl. Part. Sci., 1999, 505-556
- [9] R.Serber, Phys. Rev. 72 (1947) 1114
- [10] See e.g. the proceedings on the *5th Conference on Radioactive Nuclear Beams*, April 2000, Divonne (France), edited by Nuc. Phys. A (in press)
- [11] J.Benlliure et al., Nucl. Phys. A 660 (1999) 87
- [12] M.Blann et al., International Code Comparison for Intermediate Nuclear Data, OECD/NEA (1994)
- [13] D.Filges et al., OECD thick target benchmark, repot NCS/DOC 95 2 (1995)
- [14] B. Jurado, K.-H. Schmidt, K.-H. Behr, accepted for publication in Nuc. Phys. A
- [15] H.Geissel et al., Nucl. Inst. Meth. B 70 (1992) 286

- [16] R. Michel et al., Nucl. Ins. Meth. B 103 (1995) 183 and B 129 (1997) 153
- [17] J.P.Dufour et al., Nucl. Inst. Meth. A 248 (1986) 267
- [18] Ch.Scheidenberger et al., Nucl. Inst. Meth. B 142 (1998) 441
- [19] P.J.Karol, Phys. Rev. C 11 (1975) 1203
- [20] T.Brohm, K.-H. Schmidt, Nucl. Phys. A 569 (1994) 821
- [21] Th.Rubehn et al., Z. Phys. A 353 (1995) 197
- [22] K.-H.Schmidt et al., Nucl. Phys. A 665 (2000) 221
- [23] Y.Yariv and Z.Fraenkel, Phy. Rev. C 20 (1979) 2227
- [24] Y.Yariv and Z.Fraenkel, Phy. Rev. C 24 (1981) 488
- [25] J.Cugnon et al., Nucl. Phys. A 620 (1997) 475.
- [26] S.G.Rudstam, *Spallation of medium weight elements*, Uppsala (1956).
- [27] A.R.Junghans et al., Nucl. Phys. A 629 (1998) 635
- [28] A.V.Ignatyuk, M.G.Itkis, V.N. Okolovich, G.N.Smirenkin and A.S. Tishin, Yad. Fiz. 21 (1975) 1185 (Sov. J. Nucl. Phys. 21 (1975) 612)
- [29] P.Moller,J.R.Nix, Atom. Data Nucl. Data Tab. 59 2 (1995) 185
- [30] K.-H.Schmidt, W.Morawek, Rep. Prog. Phys. 54 (1991) 949
- [31] L.G.Moretto, Nucl. Phys. A 247 (1975) 211
- [32] A.J.Sierk, Phys. Rev. C 33 (1986) 2039
- [33] J.Benlliure et al., Nucl. Phys. A 628 (1998) 458